Kinetic Analysis of Protein Crystal Nucleation in Gel Matrix

Lei Wang*† and Xiang-Yang Liu*†
*Department of Physics, National University of Singapore, Singapore 117542; and †State Key Laboratory of Crystal Materials, Shandong University, Jinan, Shandong 250100, People's Republic of China

ABSTRACT The effect of agarose on nucleation of hen egg white lysozyme crystal was examined quantitatively using a temperature-jumping technique. For the first time, to our knowledge, the inhibition of agarose during the nucleation of lysozyme was quantified in two respects: a), the effect of increasing interfacial nucleation barrier, described by the so-called interfacial correlation parameter $f(m)$; and b), the ratio of diffusion to interfacial kinetics obtained from dynamic surface tension measurements. It follows from a dynamic surface tension analysis that the agarose network inhibits the nucleation of lysozyme by means of an enhancement of the repulsion and interfacial structure mismatch between foreign bodies and lysozyme crystals, slowing down the diffusion process of the protein molecules and clusters toward the crystal-fluid interface and inhibiting the rearrangement of protein molecules at the interface. Our results, based on ultraviolet-visible spectroscopy, also show no evidence of the supersaturation enhancement effect in protein agarose gels. The effects of nucleation suppression and transport limitation in gels result in bigger, fewer, and perhaps better quality protein crystals. The understandings obtained in this study will improve our knowledge in controlling the crystallization of proteins and other biomolecules.

INTRODUCTION

The difficulty of growing protein crystals of suitable size and high quality for x-ray crystallography is an impediment to molecular structure determination of proteins, which is necessary to explore biofunctionalities: drug design, disease treatment, controlled drug delivery, and so forth (1–3). To lower the percentage of growth defects and to control the nucleation effectively, gel crystallization is a technique currently used in crystallization of small and large macromolecules. Recently, gel crystallization has been used to mimic the conditions occurring in a microgravity environment, as the gravity-induced convection is suppressed in gel media (4).

Among the typical gel precursors used for protein crystallization, such as agarose, silica, acrylamide, or sephadex, agarose gels are the most widely used hydrogels. This is because agarose is a repetitive, essentially uncharged, marine polysaccharide, stable over a wide pH range (3.0–9.0). Unlike silica gels, it does not release any byproducts during solidification. In addition, the low gelling temperature (~28°C) of agarose makes it more suitable in view of the presence of heat-sensitive macromolecules and the condition of minimal thermal stress on proteins. In addition to the reduction of convection in the mother liquor, it is believed that agarose gel favors diffusive transport of molecules toward the crystal nuclei and the growing crystals (4,5). The gel network also traps crystal nuclei, prevents crystal sedimentation, and promotes crystal growth in three dimensions (6,7). Apart from this, agarose gels show high mechanical resistance as well as elasticity even at low agarose concentrations (<6% w/v), which provides mechanical protection during crystal soaking, mounting, and transporting (8).

As is well known, the outcome of crystallization is mainly determined by kinetic factors. In many cases, the lack of understanding in kinetics has so far prohibited the identification of robust technologies of crystal growth, in particular, the growth of biomolecules. Although some related research has recently been carried out, the understanding of the influence of gels on nucleation and crystal growth remains very poor, and the opinions concerning the role played by agarose gel in protein nucleation and growth are widely divided. For instance, some researchers suggested that the observed nucleation enhancement in agarose gels could result from the elevating of the apparent supersaturation, due to the trap of water in the agarose fiber meshes during the gelling process (9). However, this conclusion was questioned by Vidal et al. (10), who showed by small angle neutron scattering that the protein concentration and interactions were identical in gel and in gel-free media. However, lysozyme clusters of several tens to several hundreds of nanometers were noticeable in gel than in gel-free solution. Since the nuclei would be made up of some of these clusters, it was concluded that agarose gel is a nucleation promoter. Small angle x-ray scattering and gel techniques were also used to follow the kinetics of hen egg white lysozyme crystal growth (9). It follows that lowering the temperature and/or increasing the crystallizing agent concentration give rise to an increase in the attractive interactions among protein molecules in solutions while lysozyme remains monomeric. A similar behavior was observed when agarose was used. Robert et al. studied the nucleation-related phenomenon of lysozyme in gel and indicated that the formation of an amorphous precipitate in gel-free solutions never occurs in gelled solutions, which depletes the bulk

Submitted April 22, 2008, and accepted for publication September 4, 2008.
Address reprint requests to Xiang-Yang Liu, Fax: 65-6777-6126; E-mail: phyliuxy@nus.edu.sg.
Editor: Elliot L. Elson.

0006-3495/08/12/5931/10 $2.00
doi: 10.1529/biophysj.108.135574

solution (11). This could explain why the nucleation density is higher in agarose gel than in free solution. Although most reported research indicates that agarose gel promotes the nucleation of protein, the inhibition effect of agarose gel with concentration exceeding 0.4% (w/v) under a specific supersaturation was proposed by Thiessen's group (12).

To clarify the discrepancies in previous research, we present a study on the effect of agarose in protein crystal nucleation under oil (13) using an advanced temperature-jumping technique (14). Hen egg white lysozyme is used as a model protein due to its availability and relative wealth of literature. A generic kinetic model of nucleation (15,16) is applied to analyze quantitatively the effect of agarose gel on lysozyme nucleation and crystallization. In this study, the inhibition effect observed in experiments was also explained from the point of view of kinetics and interfacial structure in terms of a dynamic surface tension analysis. This analysis allows a detailed study of the kinetics of surface assembly in agarose based on a two-dimensional self-assembly mechanism.

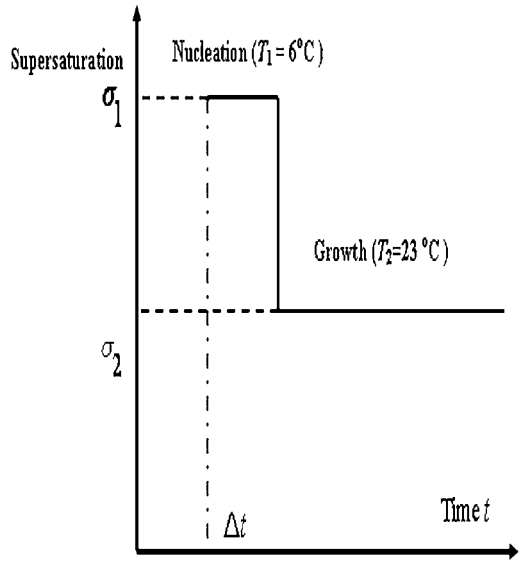

FIGURE 1 Temperature T_1 and corresponding supersaturation (σ_1) for lysozyme nucleation during the time Δt. Temperature T_2 and corresponding supersaturation (σ_2) for developing the crystals to detectable dimensions.

MATERIALS AND METHODS

Solution preparation

Hen egg white lysozyme of molecular mass ~14.3 KDa (purified six times by crystallization) was purchased from Sigma (St. Louis, MO) and used without further purification. Sodium acetate and sodium chloride, all of analytical grade, were purchased from Merck (Darmstadt, Germany). High purity deionized water (18.2 ΩM) produced by a Millipore (Billerica, MA) Milli-Q system (0.22 μm) was used for preparing buffers and solutions for protein crystallization. Sodium acetate buffer was made by titration of 0.1 M acetic acid solution with sodium hydroxide until the desired pH was obtained. The stock solutions of proteins and salts were prepared and refrigerated at 4°C for further use. Crystallization buffers and protein stock solution were filtrated by a 0.20-μm filter (Sartorius, Gottingen, Germany) before use. Sodium acetate buffer (0.1 M) containing 0.5M NaCl was used in the experiments. Lysozyme solutions were prepared by dissolving proteins in the 0.1 M sodium acetate buffer to obtain the desired concentrations of protein for the subsequent experiments at the same pH, in a 1 ml Eppendorf (Hamburg, Germany) tube. The agarose used in the experiments was Bio-Rad (Hercules, CA) certified low-melting agarose. Agarose stock solutions were prepared by dispersing the agarose powder in deionized water at room temperature and moderately stirring for 30 min and heating mixtures in a pressure vessel to 90°C for 1 h. Then, the clear agarose solution of 2% (w/v) was kept at 45°C in a thermostatic water bath for further use. In preparing lysozyme-agarose gels, the agarose stock solution, the prewarmed protein stock solution, and the buffer at 45°C were mixed to obtain the desired concentration of protein, salt, and gel (0.2% w/v). The mixture was gelled in a few minutes upon quenching temperature to $T = 23$°C.

The setup for nucleation rate determination

A strict separation between the nucleation and growth stages is the most classical method in determining the nucleation rate at a given supersaturation. A so-called temperature-jumping technique was adopted to support crystal nucleation at low temperature and crystal growth at high temperature (14,17). This technique has been in use since the 1930s, which enables the measurement of rates of nucleation experimentally, without ever actually seeing the nuclei themselves (14,17). As schematically showed in Fig. 1, at the beginning of a typical run, the protein solution is loaded at a temperature chosen to prevent nucleation. Then, the temperature is lowered to a selected T_1 at which nucleation occurs. After a period Δt, the temperature is raised from the nucleation temperature T_1 to the growth temperature T_2. In our cases, $T_1 = 6$°C and $T_2 = 23$°C. At T_2, supersaturation is at levels where the nucleation rate is practically zero, but the crystals already formed can grow to a detectable dimension. After the growth stage, the crystals nucleated at T_1 during Δt are counted under optical microscopy. The stationary nucleation rate is obtained simply by plotting the number n of crystals as a function of nucleation time Δt. A typical case indicating the time dependence of the mean number of crystals is shown in Fig. 2 with supersaturation $\sigma = 9.33$. The volume is constant in all crystallization vessels. The period Δt should not be too long to avoid Ostwald ripening. The boundary between conditions causing nucleation or precipitation, and the conditions yielding a clear solution, can be determined by screening of crystallization conditions at 6°C and 23°C. The solubility data of lysozyme were obtained from Howard et al. (18) and Cacioppo and Pusey (19).

In our experiments, 22 mg/ml–28 mg/ml lysozyme with 0.5M NaCl concentration in 0.1M NaAc buffer at PH = 4.5 with 1–2 mg/ml intervals that have supersaturation between 9% and 13% were used in the process of experiment. These hen egg white lysozyme solutions are known to be metastable at 23 ± 0.5°C by the above-mentioned screening experiments. Rapid nucleation occurred in <30 min at the selected range of supersaturation.

The nucleation experiments were conducted using 72 well Terazaki plates (Hampton Research, Alisa Viejo, CA) in an EYELA (Tokyo, Japan) KCL-2000 incubator. The microbatch method allowed us to obtain an exact initial supersaturation value, which can be used in our nucleation kinetic study. The Terazaki plates were thoroughly rinsed with deionized water to remove dust particles and impurities. During filling, the dried plates were set on a damp paper towel to prevent static electricity buildup. To minimize the evaporation of solution and suppress the undesired nucleation on the solution surface, the aqueous solution samples were dispensed and incubated under the surface of inert silicon oil (AS4 from Sigma).The solutions were quickly dispensed to a row of 12 wells on the plate. Then the plates were sealed with clear tape and moved into a precooled incubator. The incubator temperature was preset at 6°C for crystal nucleation. At the end of the preset regular nucleation time, the plates were kept in a thermostat at 23°C. For all of the experiments conducted in this study, a fixed solution volume of 0.4 μl per well was used. As nucleation is expected to be a stochastic process, for each plate, 12 wells per sample were used to provide a broad range of sampling results (20).

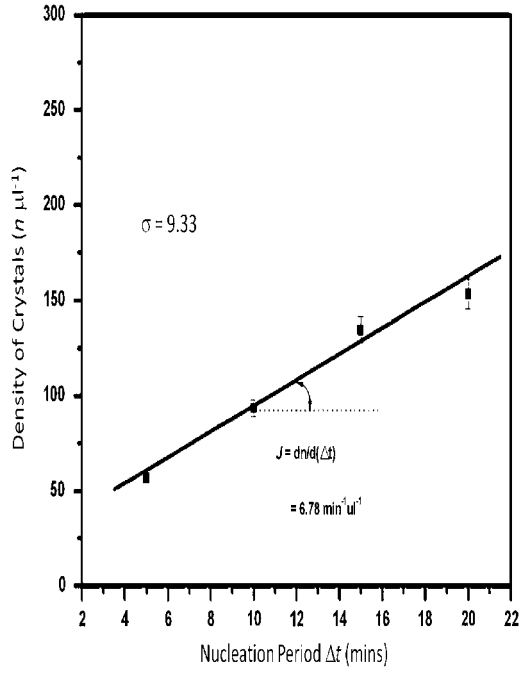

FIGURE 2 Time dependence of the mean number of crystals per microliter at the supersaturation of 9.33 at 6°C.

Because of oil sealant, the water loss in the process of experiments can be negligible (20). The time for changing of temperature from T_2 to T_1 and from T_1 to T_2 is determined by the thermal properties of the materials from which the crystallization container is built. Nevertheless, the quenching period (~30 s) is much shorter than the nucleation induction period. The shortest Δt was 5 min. Therefore, we can regard the temperature drop from T_2 to T_1 as an instant event, and the quenching period has not much influence on the crystallization kinetics examined in this study.

The observations were performed under a polarized transmitted microscope (Olympus (Tokyo, Japan) BX60-F) with an attached 3CCD color video camera (Panasonic (Tokyo, Japan), KY-F55BE), which is combined with a computer to record the image of each well. At a later time, analySIS 3.0 software from Soft Imaging System GmbH (Munster, Germany) was used to process images and to manually tag and count the crystals. To ensure the applicability of the data, experiments were conducted in duplicate and occasionally in triplicate.

Measurements of surface tension and ultraviolet-visible spectra

The dynamic surface tension was determined using the Wilhelmy plate method with a Sigma 700 tensiometer (Helsinki, Finland). The measurements were performed at 6°C controlled by a thermostatic water bath. For a typical measurement, an appropriate volume of lysozyme stock solution was added to keep the protein concentration constant at the supersaturation of 9.8% with or without 0.2% (w/v) agarose. The surface tension decreases with time before reaching an equilibrium value. The experimental sample chamber was saturated with pure water vapor to keep a consistent humid environment. All the containers used in this experiment were cleaned by chromic acid to eliminate potential organic contaminations.

The ultraviolet-visible (UV-Vis) absorption spectra of diluted lysozyme solutions with and without 0.2% (w/v) agarose were measured on a VARIAN (Palo Alto, CA) Cary 50 UV-Vis spectrophotometer using a quartz cuvette having 1-cm path length at the nucleation temperature.

RESULTS AND DISCUSSION

Kinetic model for lysozyme nucleation

In this section, a heterogeneous kinetics model (15,16) is adopted to examine the nucleation of lysozyme. Nucleation, the birth of protein crystals, means overcoming a free energy barrier, the so-called nucleation barrier (ΔG^*) at a given thermodynamic driving force $\Delta\mu$(15,16,21), resulting in a continuous increase in the size of crystalline clusters. Recent research suggests that if the interfacial free energy between the crystal and the fluid phase is not too low, the nucleation is normally controlled by a number of heterogeneous nucleation processes, as supersaturation increases (22–24).

By taking into account the influence of foreign bodies (dust particles, or the walls of crystallization vessel) on the nucleation process, the nucleation rate of lysozyme, which is defined as the number of nuclei generated per unit time per unit volume, is given based on the model by Eqs. 1–4 (15,16,25):

$$J = (R^s)^2 N^0 f''(m)[f(m)]^{1/2} B' \exp\left[-\frac{\Delta G^*_{\text{homo}}}{kT} f(m)\right] \quad (1)$$

with

$$\Delta G_{\text{homo}} = \frac{16\pi\gamma_{\text{cf}}^3\Omega^2}{3[kT\ln(1+\sigma)]^2} \quad (2)$$

$$f''(m) = \frac{1}{2}(1-m) \quad (3)$$

$$f(m) = \frac{1}{4}(2-3m+m^3), \quad (4)$$

where B' is the kinetics constant, γ_{cf} denotes the specific interfacial free energy between the crystals and the mother phase, Ω is the volume of each growth units, and R^s and N^0 are the radius of curvature and the density of foreign bodies, respectively. k is Boltzmann's constant and T is the absolute temperature. The supersaturation σ is defined as

$$\sigma = (C - C_e)/C_e, \quad (5)$$

where C and C_e are the actual and equilibrium concentration, respectively.

In Eqs. 3 and 4, m depends on the interaction and the structural match between the nucleating phase and foreign bodies, and is a function of the interfacial free energy among the different phases:

$$m = (\gamma_{\text{sf}} - \gamma_{\text{sc}})/\gamma_{\text{cf}} \approx \cos\theta\ (-1 \le m \le 1), \quad (6)$$

where γ_{sf}, γ_{sc}, and γ_{cf} correspond to the interfacial tensions between substrate and fluid, between crystal and substrate, and between crystal and fluid, respectively. θ is the contact angle between the nucleating phase and the substrate. Notice that $f(m)$ is a factor describing the lowering of the nucleation barrier ΔG^* due to the occurrence of foreign bodies (or substrate):

$$f(m) = \Delta G^*/\Delta G^*_{\text{homo}}. \quad (7)$$

In this equation, ΔG^* is the actual nucleation barrier and ΔG^*_{homo} is the homogeneous nucleation barrier.

Obviously, this factor plays an important role in the determination of the heterogeneous nucleation barrier. If $m \rightarrow -1$, then $f(m) \rightarrow 1$ (cf. Eq. 4), the interaction and structural match between the nuclei and the substrates are very poor. Foreign bodies exert almost no influence on nucleation. On the contrary, if the interaction between the nucleating phase and the substrate is optimal, one has $m \rightarrow 1$ and $f(m) \rightarrow 0$ (cf. Eq.4). It follows that crystals only occur at the surface of foreign bodies, and the growth of crystals, guided by the structure of the substrate, will be compact and well orientated.

Combining and rearranging Eqs. 1, 2, and 7 yield Eq. 8,

$$\ln J = -\frac{\kappa f(m)}{[\ln(1+\sigma)]^2} + \ln\left\{(R^s)^2 N^0 f''(m)[f(m)]^{1/2} B'\right\} \quad (8)$$

with

$$\kappa = 16\pi\gamma_{cf}^3 \Omega^2 / 3(kT)^3. \quad (9)$$

The aforementioned effects can be identified from the plot of $\ln J \sim 1/[\ln(1+\sigma)]^2$, which will give rise to a straight line for a given heterogeneous nucleation process. Obviously, for a given system (κ, B' are constants) the slope and interception of the straight line will change accordingly with $f(m)$.

As the substrate, foreign bodies always lower the nucleation barrier by a factor of f (cf. Eq. 7). As illustrated in Fig. 3, in the case of nucleation promotion (transition from curve 0 to curve 1), the adsorption of additives on the original substrate will modify the interaction and structural match between the substrate (foreign bodies) and the nucleating phase. This will then result in a change in the nucleation barrier. Since for a given nucleation system, κ is constant, any change in the nucleation barrier can then be identified from the increase of the slope ($-\kappa f(m)$) and the intercept ($\ln\{(R^s)^2 N^0 f''(m)[f(m)]^{1/2} B'\}$)of the $\ln J \sim 1/[\ln(1+\sigma)]^2$ plot (cf. Eq. 8). The nucleation inhibition effect can be identified from the decrease in the slope (($-\kappa f(m)$) of $\ln J \sim 1/[\ln(1+\sigma)]^2$ plot (cf. *curve 0* to *curve 2* in Fig. 3) and/or the decrease of the intercept of $\ln J \sim 1/[\ln(1+\sigma)]^2$ plot. This is due to the repulsion and an interfacial structure mismatch between the substrate and the nucleating phase caused by the adsorption of additives, which reduces the positive effect of substrate in the nucleation barrier lowering. On the other hand, the promotion effect of additives on nucleation kinetics can be identified from the increase in the slope ($-\kappa f(m)$) of $\ln J \sim 1/[\ln(1+\sigma)]^2$ plot (cf. *curve 0* to *curve 1* in Fig. 3) and/or the enhancement of the intercept of $\ln J \sim 1/[\ln(1+\sigma)]^2$ plot. Therefore, in the following discussion, we can apply these parameters to analyze the effect of agarose on the kinetics of lysozyme nucleation.

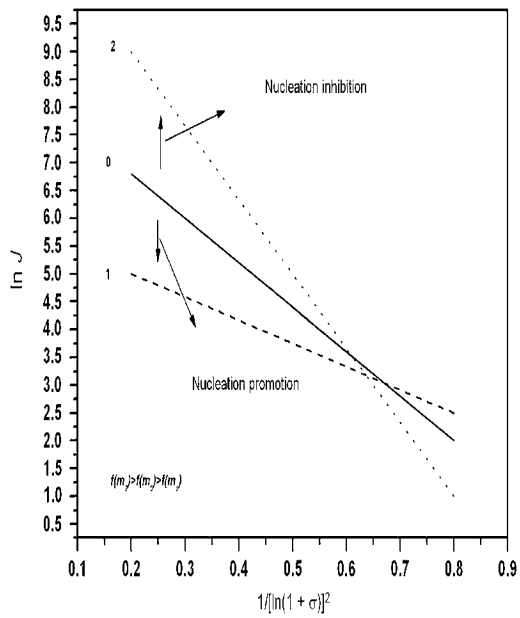

FIGURE 3 Effect of additives on the interfacial correlation factor $f(m)$ and the nucleation kinetics. A promotion or inhibition effect will increase or decrease the interfacial correlation parameter in the plot of $\ln J \sim 1/[\ln(1+\sigma)]^2$.

Dynamic surface tension analysis for diffusion versus interfacial kinetics

We notice that nucleation is not only determined by the influence of foreign bodies on the nucleation barrier as aforementioned, but also by the diffusion process and the molecular surface integration process.

As is well known, the growth of protein crystals is normally governed by layer-by-layer mechanism (15,16,26,27). This implies that the growth of three-dimensional (3D) protein crystals is accomplished by a sequence of two-dimensional (2D) nucleation and spread forming a 2D crystal layer on an existing crystal surface (15,16). We notice that the layer-by-layer growth of crystals can also be governed by a spiral mechanism as well (15,16,26,27). The spiral mechanism normally governs the layer-by-layer growth of crystals at relatively low supersaturations, whereas the 2D nucleation mechanism governs the growth of crystals at high supersaturations. In fact, very high supersaturations are typically used for growing protein crystals. Therefore, we will mainly focus on the 2D nucleation mechanism in the case of protein crystallization.

Between the two steps of the ''birth'' and ''spread'' process of 2D nucleation growth (15,16), the formation of a 2D crystal can be used as an analogy for the formation of a new layer of a crystal on an existing growing crystal surface. Our recent research indicated that the protein 2D self-assembly on the surface of an aqueous solution shares the similar structure of the 3D crystal structure (28). This 2D surface with the self-assembled protein layer can act as a self template for the 3D protein crystallization or treated as a model surface of growing protein crystals. This approach provides us with

what we believe is a new and simple method of studying the interfacial kinetics of protein crystallization.

Like all amphiphilic molecules, proteins tend to self-assemble at the air/solution interface and therefore lower the surface tension (29). So the dynamics of surface tension reflects the kinetics of the 2D self-assembly of proteins at the interface.

As shown in Fig. 4, the rate of reduction of surface tension is determined by three consecutive processes: At the early stage of surface assembly, there is no energy barrier between the surface and subsurface. At this stage, diffusion is the rate-determining factor (Fig. 4 *a*). The surface tension is given by

$$\gamma(t) = \gamma_0 - 2C_p kT\left(\frac{D}{3.142}t\right)^{1/2}, \tag{10}$$

where $\gamma(t)$ is the surface tension at time t, γ_0 the solvent surface tension, C_p the bulk protein concentration, and D the diffusion coefficient of protein molecules. In this step, the plot of γ against $t^{1/2}$ will be linear.

At higher surface coverage, there are energy barriers to penetration of molecules into the surface. In this step, penetration is the rate-determining factor (Fig. 4 *b*). When the surface is almost fully occupied, the reduction of surface tension will be determined by the molecular rearrangement in the adsorption layer (Fig. 4 *c*). For the situation where there is an energy barrier to assembly, Eq. 9 can be modified to give

$$\ln\frac{d\Pi(t)}{dt} = \ln(\bar{k}C_p) - \Pi(t)\Delta A/kT, \tag{11}$$

where $\Pi(t) = \gamma_0 - \gamma(t)$ is the surface pressure at time t, $\bar{k}$ is a constant related to the adsorption ability, and ΔA represents the mean area created in the film to adsorb a protein molecule.

When protein molecules penetrate into the interfacial region they affect the surface free energy. Since in polymer adsorption the first layer effects are dominant in determining Π, changes in Π provide a convenient way of monitoring the penetration into the surface and the configurationally rearrangements of the adsorbed protein molecules. The last two processes can be called surface integration. The rate of the above mentioned processes can be analyzed by the first-order equation (29)

$$\ln\left(1 - \frac{\Pi(t)}{\Pi_e}\right) = -\frac{t}{\tau}, \tag{12}$$

where Π_e and $\Pi(t)$ are the surface pressure values in the equilibrium state and at any time t for measurement, respectively. τ denotes the relaxation time of the related kinetic processes. Therefore, the rate constant, k_i $(= 1/\tau_i; i = d, p, r,$ denoting for diffusion, penetration, rearrangement, respectively), represents the rate at each kinetic step, which can be obtained from the slope of the $\ln(1 - (\Pi(t)/\Pi_e)) \sim t$ plot at the different stages. The detailed analyses can be referred to references 28, 30, 31, and 32.

We notice

$$\tau \propto \exp\left(\frac{\Delta G}{k_B T}\right), \tag{13}$$

where ΔG is the kinetics energy barrier from one state to another in the process of protein crystallization. Evidently, a faster relaxation rate k_i or shorter relaxation time τ corresponds to a lower energy barrier based on Eq. 13 and vice versa (33).

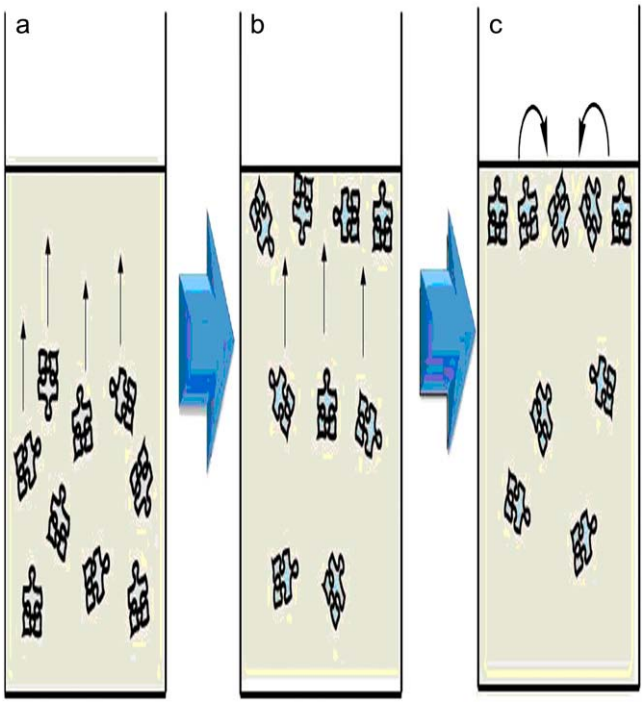

FIGURE 4 Protein 2D interface assembly kinetics. (*a*) The diffusion of protein molecules to the interface. (*b*) The penetration of protein molecules through the interface film from subsurface (a thickness of a few molecular diameters next to surface) to the surface (28). (*c*) Molecular rearrangements of adsorbed molecules in the film.

Nucleation kinetics analysis for agarose effect of on lysozyme nucleation

Under the specific range of supersaturation, the role of the substrate (or foreign bodies) is an important factor that influences the interfacial properties. Although the occurrence of a substrate will promote nucleation by decreasing the nucleation energy, it will also exert a negative impact on the surface integration. The substrate will reduce the effective collisions of structure units with the surface of the nucleating clusters, which slows down the nucleation kinetics. This is the so-called shadow effect of substrate, described by the term $\{(R^s)^2 N^0 f''(m)[f(m)]^{1/2} B'\}$ in Eqs. 1 and 8 (15,16). At very higher supersaturations, where the nucleation barrier

becomes essentially low, the effective collisions will dominate in controlling the kinetics. The occurrence of substrate will then slow down the nucleation kinetics.

As mentioned earlier, the resultant effect of additives can be decided by the changes of slope and intercept of the $\ln J \sim 1/[\ln(1+\sigma)]^2$ plot. The interfacial correlation factor $f(m)$ can characterize the effect of agarose on lysozyme nucleation and the structure correlation between the nucleating lysozyme crystal sand foreign bodies. As shown in Fig. 5, on the basis of Eq. 7, both plots (with and without agarose) give rise to two straight lines with different slopes and intercepts in the limited range of supersaturation. The slopes, intercepts and related parameters obtained from a linear regression are given in Table 1. The details for calculating $\kappa_{aga}/\kappa, f(m)_{aga}/f(m)$, and $\Delta G^*_{aga}/\Delta G^*$ from the slope and the intercept of the $\ln J \sim 1/[\ln(1+\sigma)]^2$ plot can be obtained from related references (15,16,27,34). In Fig. 5, a comparison of the straight lines shows that the existence of agarose gel results in a decrease in the slope of the $\ln J \sim 1/[\ln(1+\sigma)]^2$ plot from -20.9215 to -36.165 and an increase in the intercept from 6.9624 to 8.5323 (cf. Fig. 5 and Table1). These two effects are essentially opposite. Nevertheless, within the range of experimental supersaturations, the plot of $\ln J \sim 1/[\ln(1+\sigma)]^2$ for the solutions with agarose gel is below that without agarose gel; therefore, the nucleation inhibition effect of agarose gel dominates. In the following section, it will be shown that $\kappa_{aga}/\kappa \approx 1.15$; one has then $f(m)$ of curve 1′ is larger than that of curve 1 by a factor of 1.49 ($f(m)_{aga}/f(m) \cong 1.49$). This indicates that the presence of agarose leads to an interfacial structure mismatch between the foreign particles and lysozyme crystals, due to the adsorption of agarose molecules on the foreign bodies, illustrated by Fig. 6. This adsorption of agarose molecules on the foreign bodies lifts the nucleation barrier, resulting in a reduction in the total nucleation number. Therefore, it can be seen later that bigger and fewer regular crystals can be obtained from gels.

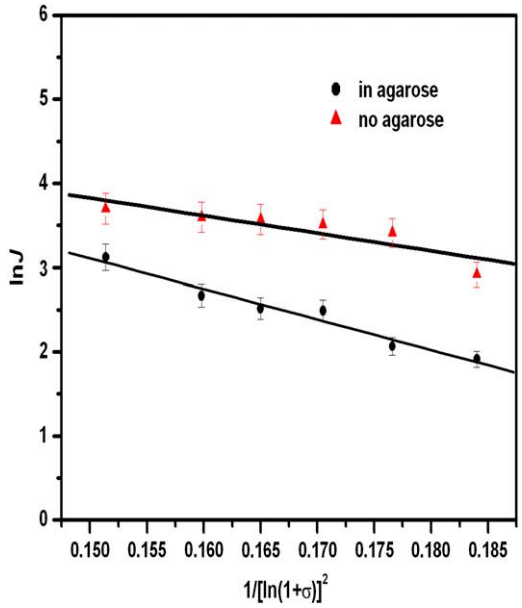

FIGURE 5 Influence of agarose on the nucleation kinetics of lysozyme at pH = 4.5, 6°C. Schematic plot of $\ln J \sim 1/[\ln(1+\sigma)]^2$ with error bar.

Dynamic surface tension analysis for agarose gel related inhibition effect

To explain the molecular origin of the changes in lysozyme nucleation kinetics in the presence of agarose, dynamic surface tension measurements were performed at a temperature of 6°C. The results are given in Fig. 7. Based on the data in Fig. 7, we plotted $\ln(1-\Pi(t)/\Pi_e)$ versus t in Fig. 8. The three mutually intercepted straight lines for each case indicates that the dynamics of protein assembly at the air-water interface follows three consecutive steps: diffusion, penetration, and rearrangement, as discussed before. The rate constant of each straight line can be obtained from the slope of the segment by linear regression, as shown in Table 2.

Compared with lysozyme in gel-free solution, the surface tension profiles for the lysozyme/agarose system are shifted upward (Fig. 7). According to the Gibbs equation (25),

$$\Gamma = -\frac{1}{R_g T}\frac{d\gamma}{d\ln a}, \tag{14}$$

where Γ is the amount of surfactant adsorbed at the interface, R_g is the gas constant, γ is the surface tension, and a is the surfactant activity. The surface tension decreases in pro-

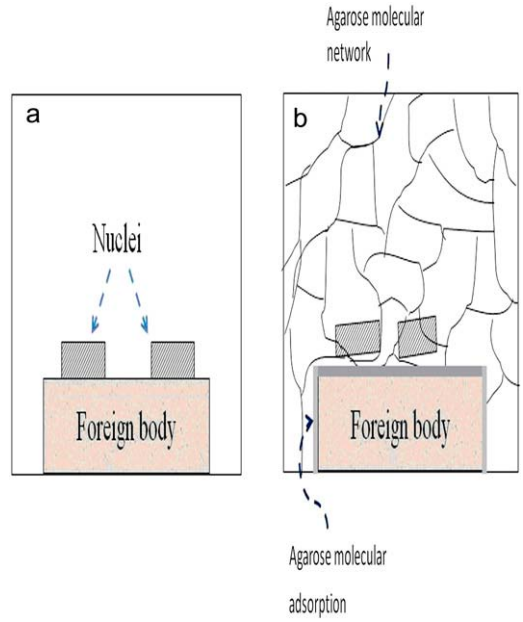

FIGURE 6 Schematic drawing of structural match between the nucleating phase and foreign bodies (*a*) in gel-free solution and (*b*) in gel solution. The gel fibers separate the foreign bodies and nuclei and lead to the structure mismatch between the two phases.

TABLE 1 Effect of agarose on the interfacial effect parameter and energy barrier for the nucleation of lysozyme

Curve	$-\kappa f$*	$B^{\dagger}$	$\kappa_{aga}/\kappa^{\ddagger}$	$f(m)_{aga}/f(m)$	$\Delta G^*_{aga}/\Delta G^{*\S}$
1 (without agarose)	−20.9215	6.9624	—	—	—
1′ (with agarose)	−36.165	8.5323	1.16	1.49	1.49

*$-\kappa f$ is the slope of the curve.
†B is the intercept of the curve.
‡κ_{aga} is κ in agarose.
§$\Delta G^*_{aga}/\Delta G^* = f(m)_{aga}/f(m)$.

portion to the amount of surfactant adsorbed at the interface. When agarose is added, the number of proteins being adsorbed on the solution surface decrease, as some proteins becomes trapped in the network of agarose. Therefore, the surface tension in agarose is higher than that in gel-free solution, and the surface free energy in the presence of agarose will increase from $\gamma_{fg} = 54.82$ mN/m to $\gamma'_{fg} = 57.59$ mN/m. If we adopt the proportional approximation (35), the following relationship will be obtained:

$$\frac{\gamma_{cf}}{\gamma'_{cf}} \sim \frac{\gamma_{fg}}{\gamma'_{fg}}. \tag{15}$$

If γ_{cf} and γ'_{cf} denote the interfacial tension between crystal and the aqueous solution and gel, Eq. 15 will give rise to $\gamma'_{cf}/\gamma_{cf} \approx 1.05$. Based on the definition of κ (Eq. 9), κ will increase by a factor of 1.15 when nucleation occurs in agarose gels ($\kappa_{aga}/\kappa \approx 1.15$).

In Table 2, the bulk diffusion constant k_d, the molecular penetration constant k_p, and the molecular rearrangement rate

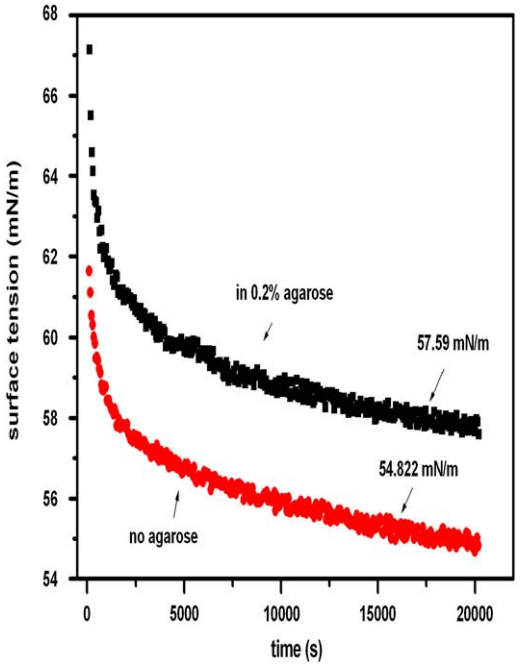

FIGURE 7 Typical figure of surface tension of lysozyme solution at the air/water interface as a function of time at 6°Cfor selected values of supersaturation

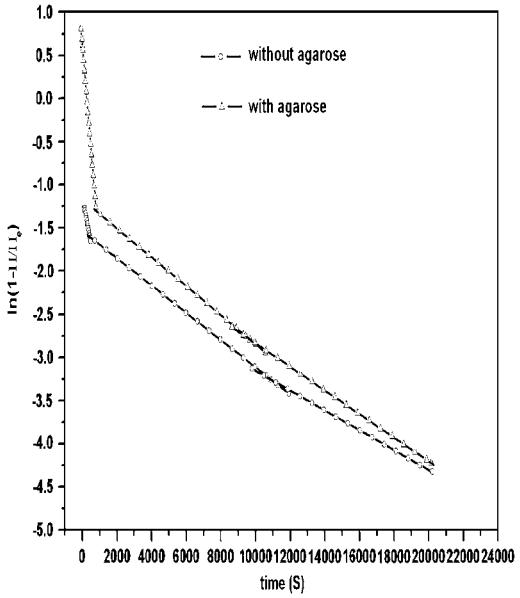

FIGURE 8 $\ln(1 - \Pi/\Pi_e)$ as a function of time for lysozyme with and without 0.2% agarose. The rate constants for different steps can be obtained from the slope of the linear regression parts.

constant k_r of protein molecules at the interfacial layer are given for the diluted lysozyme solutions with and without agarose. These data allow us to obtain more information at the molecular level during the crystallization process. As shown in Table 2, the diffusion of lysozyme molecules through the agarose molecule network in the gels is slower than through aqueous solutions. Because the mobility of lysozyme molecules in the gel media is obstructed by the entangled agarose network, the diffusion step is slowed down (cf. Fig. 6). The k_p shows that the agarose gels do not have much influence on the penetration of lysozyme molecules into the interfacial layer. During the penetration, the distance of a few molecular diameters makes the impact of agarose gel less significant. The slight change of the surface integration rate would be understandable. On the other hand, the occurrence of agarose molecules will hinder the rearrangement of lysozyme molecules at the interface, as agarose and lysozyme molecules may interact with each other. In order words, lysozyme molecules are to some extent bounded to the agarose molecule network.

TABLE 2 Rate constant of diffusion, penetration and rearrangement

Curve	γ_{fg}* (mN/m)	$k_d{}^{\dagger}$ ($\times 10^{-4} S^{-1}$)	$k_p{}^{\ddagger}$ ($\times 10^{-4} S^{-1}$)	$k_r{}^{\S}$ ($\times 10^{-4} S^{-1}$)
2 (without agarose)	54.822	10.6	1.33	2.25
2′ (with agarose)	57.59	8.53	1.52	1.65

*Surface tension at air-water interface.
†Diffusion rate constant.
‡Penetration rate constant.
§Rearrangement rate constant.

We notice it is well known that convection can be suppressed by gel networks; our results of the suppression of lysozyme molecule diffusion and the inhibition of the macromolecular rearrangement at the interface are quite surprising. This will actually exert a direct impact on the quality and mass crystallization of proteins, which will be discussed in the following section.

Nucleation Inhibition verified by optical microscopy

Fig. 9, *a* and *b*, shows lysozyme crystals grown in a gel-free solution, and in a gelled solution (0.2% w/v), respectively. The two solutions have the same concentration of precursor (22 mg/ml, 0.5 MNaCl, pH = 4.5) and the same nucleation and growth duration. Compared with the solution grown crystals (Fig. 9 *a*), the gel-grown crystals form a uniform population with a bigger size and fewer and more regular crystals. In 0.2% agarose gel, the sedimentation of crystals was obviously prevented and the secondary nucleation of lysozyme was also suppressed. We notice that lysozyme crystals grown from agarose gels are more regular and contain fewer inclusions. The above observations can be understood based on the results obtained in the previous sections. A uniform size distribution and the big size of protein crystallites are attributed to the suppression of protein nucleation. The more regular lysozyme crystals with less inclusions when growing from agarose gels can be attributed to the transport (both diffusion and convection) limitation of lysozyme clusters toward the growing surfaces of lysozyme crystals through agarose molecular networks, which prevents the occurrence of defects (mainly inclusions) during crystallization. Although more data are needed to draw a final conclusion, better quality protein crystals could be expected when grown from agarose gels.

Verification of supersaturation enhancement effect in agarose gel nucleation

The supersaturation enhancement effect in agarose has been widely accepted as the main reason for the nucleation promotion phenomenon discussed in many articles (36). According to the published results, the meshes of agarose molecular networks trap water during the gelling process, causing higher actual concentrations than the corresponding gel-free solutions (9). Nevertheless, the Vidal group's results showed otherwise (10). To check whether there is such a supersaturation enhancement effect, we carried out UV-Vis spectroscopic measurements for the solutions as mentioned in the Materials and Methods section. According to the Beer-Lambert law, the lysozyme concentration in the diluted solution can be obtained from absorbance at 280 nm in UV-Vis spectra (Fig. 10). In our measurements under the nucleation temperature, the spectrum in agarose is almost the same as that in the gel-free solution. The very similar absorbance between the gelled and gel-free solutions at 280 nm supports the Vidal group's results based on small angle neutron scattering (10), which show that the concentration and supersaturation of protein are identical in both gel and gel-free media. Both the Vidal group's and our results eliminate the possibility of the aforementioned supersaturation enhancement effect.

We notice that a better understanding and control of the gel related crystallization are very relevant in the crystallization

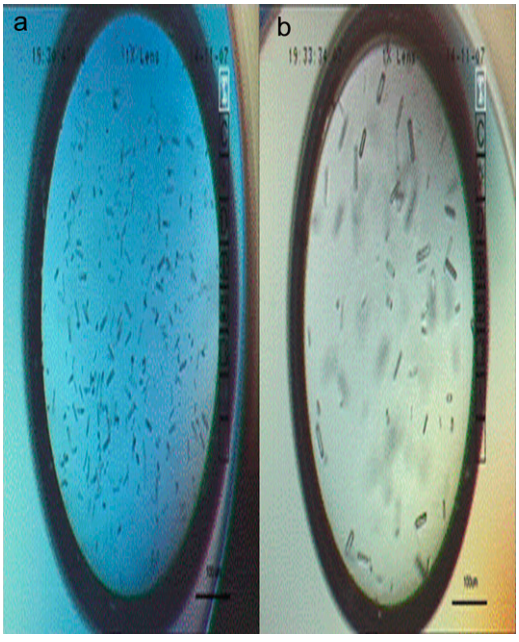

FIGURE 9 Lysozyme crystals in gel-free (*a*) and gelled (*b*) 0.4 μl microbatch drops under oil.

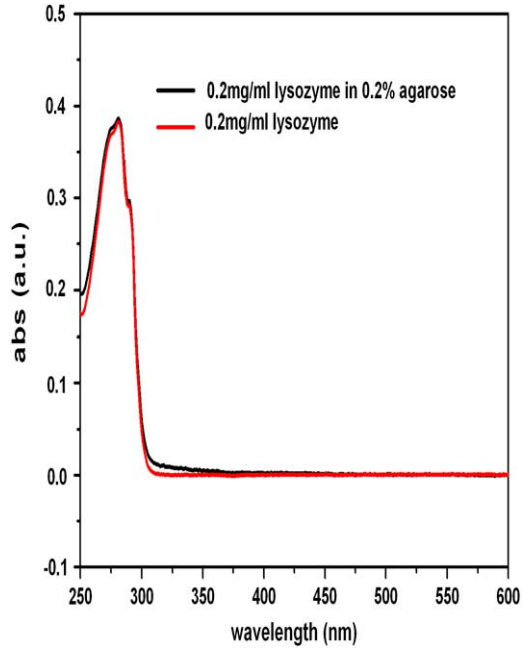

FIGURE 10 UV-Vis spectra of diluted lysozyme solution in the presence of 0.2% agarose gel and in the absence of agarose gel.

of proteins and other biomolecules. Better quality crystals induced by the nucleation and transport suppression in gel will result in a more accurate determination of protein 3D structures. This could lead to a more precise understanding of biological function of proteins and improved drug design in applications of structure biology application (37). The production of crystals of a relatively uniform size due to nucleation suppression and transport limitation in gel will enable required dosages to be prescribed correctly, an important step in achieving controlled drug delivery. In addition, in the pharmaceutical industry, the control of polymorphism and the size of the crystals will directly affect the bioefficacy and bioavailability of the drugs (38). In addition, a uniform size distribution and a big size of protein crystallites are ideal for protein storage and transport.

SUMMARY AND CONCLUSIONS

In summary, we have studied the nucleation kinetics of lysozyme and quantified the effect of agarose on lysozyme nucleation based on a heterogeneous nucleation model and an interfacial kinetics model. The inhibition effect in gel was also distinguished quantitatively by the ratio of the diffusion and surface integration based on the protein 2D interface assembly kinetics. Both the experimental data of nucleation kinetics and interfacial kinetics demonstrate that agarose molecules give rise to the interfacial structure mismatch between the substrate and the nucleating lysozyme crystals, and trap the protein molecules and the clusters in the diffusion process and inhibit the rearrangement of protein molecules at the interface. Our results also support the argument that the concentration and supersaturation of proteins are identical in both gel and gel-free media. These effects result in bigger and fewer protein crystals with perhaps better quality and a uniform size distribution. These findings will facilitate identifying robust technologies in controlling the crystallization of biomacromolecules.

This work was supported by Singapore Academic Research Funds R-144-000-139-112, R-144-000-169-101, and R-144-000-169-112.

REFERENCES

1. McPherson, A. 1999. Crystallization of Biological Macromolecules. Cold Spring Harbor Press, Cold Spring Harbor, NY.
2. Matsuda, S., T. Senda, S. Itoh, G. Kawano, H. Mizuno, and Y. Mitsui. 1989. New crystal form of recombinant murine interferon-β. *J. Biol. Chem.* 264:13381–13382.
3. Hirsch, R. E., C. Raventos-Suarez, J. A. Olson, and R. L. Nagel. 1985. Ligand state of intraerythrocytic circulating HbC crystals in homozygote CC patients. *Blood.* 66:775–778.
4. Lorber, B., and R. Giegé. 2001. Nucleation and growth of thaumatin crystals within a gel under microgravity on STS-95 mission vs. under Earth's gravity. *J. Cryst. Growth.* 231:252–261.
5. Moreno, A., B. Quiroz-García, F. Yokaichiya, V. Stojanoff, and P. Rudolph. 2007. Protein crystal growth in gels and stationary magnetic fields. *Cryst. Res. Technol.* 42:231–236.
6. Sauter, C., B. Lorber, and R. Giegé. 2002. Towards atomic resolution with crystals grown in gel: the case of thaumatin seen at room temperature. *Proteins.* 48:146–150.
7. Robert, M. C., and F. Lefaucheux. 1988. Crystal growth in gels: principle and applications. *J. Cryst. Growth.* 90:358–367.
8. Biertümpfel, C., J. Basquin, D. Suck, and C. Sauter. 2002. Crystallization of biological macromolecules using agarose gel. *Acta Crystallogr. D Biol. Crystallogr.* 58:1657–1659.
9. Finet, S., F. Bonneté, J. Frouin, K. Provost, and A. Tardieu. 1998. Lysozyme crystal growth, as observed by small angle X-ray scattering, proceeds without crystallization intermediates. *Eur. Biophys. J.* 27:263–271.
10. Vidal, O., M. C. Robert, and F. Boué. 1998. Gel growth of lysozyme crystals studied by small angle neutron scattering: case of agarose gel, a nucleation promoter. *J. Cryst. Growth.* 192:257–270.
11. Robert, M. C., Y. Bernard, and F. Lefaucheux. 1994. Study of nucleation-related phenomena in lysozyme solution. Application to gel growth. *Acta Crystallogr. D Biol. Crystallogr.* 50:496–503.
12. Thiessen, K. J. 1994. The use of two novel methods to grow protein crystals by mierodialysis and vapor diffusion in an agarose gel. *Acta Crystallogr. D Biol. Crystallogr.* 50:491–495.
13. Moreno, A., E. Saridakis, and N. E. Chayen. 2002. Combination of oils and gels for enhancing the growth of protein crystals. *J. Appl. Cryst.* 35:140–142.
14. Tsekova, S., S. Popova, and C. Nanev. 2002. Nucleation rate determination by a concentration pulse technique: application on ferritin crystals to show the effect of surface treatment of a substrate. *Acta Crystallogr. D Biol. Crystallogr.* 58:1588–1592.
15. Liu, X. Y. 2001. Generic mechanism of heterogeneous nucleation and molecular interfacial effects. *In* Advances in Crystal Growth Research. K. Sato, K. Nakajima, and Y. Furukawa, editors. Elsevier Science, Amsterdam, The Netherlands. 42–61.
16. K.-Q. Zhang and X. Y. Liu, 2004. In situ observation of colloidal monolayer nucleation driven by an alternating electric field. *Nature.* 429:739–742.
17. Penkova, A., N. Chayen, E. Saridakis, and C. N. Nanev. 2002. Nucleation of protein crystals in a wide continuous supersaturation gradient. *Acta. Crys.* D58:1606–1610.
18. Howard, S. B., P. J. Twigg, J. K. Baird, and E. J. Meehan. 1988. The solubility of hen egg-white lysozyme. *J. Cryst. Growth.* 90:94–104.
19. Cacioppo, E., and M. L. Pusey. 1991. The solubility of tetragonal form of hen egg white lysozyme from pH 4.0 to 5.4. *J. Cryst. Growth.* 114:286–292.
20. Judge, R. A., R. S. Jacobs, T. Frazier, E. H. Snell, and M. L. Pusey. 1999. The effect of temperature and solution pH on the nucleation of tetragonal lysozyme crystals. *Biophys. J.* 77:1585–1593.
21. Zettlemoyer, A. C. 1969. Nucleation. Marcel Dekker, New York.
22. Liu, X. Y., and S. W. Lim. 2003. Templating and supersaturation-driven anti-templating: principles of biomineral architecture. *J. Am. Chem. Soc.* 125:888–895.
23. Liu, X. Y. 2000. Generic progressive heterogeneous processes in nucleation. *Langmuir.* 16:7337–7345.
24. Liu, X. Y., and C. S. Strom. 2000. Self-epitaxial nucleation origin of fractal aggregation. *J. Chem. Phys.* 113:4408–4411.
25. Liu, X. Y. 2000. Heterogeneous nucleation or homogeneous nucleation? *J. Chem. Phys.* 112:9949–9953.
26. Land, T. A., A. J. Malkin, Y. G. Kuznetsov, A. Mcpherson, and J. J. Deyoreo. 1995. Mechanisms of protein crystal growth: an atomic force microscopy study of canavalin crystallization. *Phys. Rev. Lett.* 75: 2774–2777.
27. Liu, X. Y., K. Maiwa, and K. Tsukamoto. 1997. Heterogeneous two-dimensional nucleation and growth kinetics. *J. Chem. Phys.* 106:1870–1879.
28. Jia, Y. W. 2005. Self-assembly of protein at aqueous solution surface in correlation to protein crystallization. *Appl. Phys. Lett.* 86:023903–1–023903–3.
29. Magdassi, S., and O. Toledano. 1996. Enhanced hydrophobicity: formation and properties of surface-active proteins. *In* Surface Activity

of Proteins: Chemical and Physicochemical Modifications. S. Magdassi, editor. Marcel Dekker, New York. 39–60.

30. Ward, A. F. H., and L. Tordai. 1946. Time-dependence of boundary tensions of solutions I. The role of diffusion in time-effects. *J. Chem. Phys.* 14:453–461.
31. Subirade, M., and J. Gueguen. 1992. Effect of dissociation and conformational changes on the surface behavior of pea legumin. *J. Colloid Interface Sci.* 152:442–454.
32. Tornberg, E. 1978. The application of the drop volume technique to measurements of the adsorption of proteins at interfaces. *J. Colloid Interface Sci.* 64:391–402.
33. Jia, Y. W., and X. Y. Liu. 2006. From surface self-assembly to crystallization: prediction of protein crystallization conditions. *J. Phys. Chem. B.* 110:6949–6955.
34. Liu, X. Y. 1999. A new kinetic model for three-dimensional heterogeneous nucleation. *J. Chem. Phys.* 111:1628–1635.
35. Liu, X. Y. 1993. The solid-fluid interface: a comparison and further description using the layer model. *Surf. Sci.* 290:403–412.
36. Provost, K., and M. C. Robert. 1995. Crystal growth of lysozymes in media contaminated by parent molecules: influence of gelled media. *J. Cryst. Growth.* 156:112–120.
37. Zheng, B., L. S. Roach, and R. F. Ismagilov. 2003. Screening of protein crystallization conditions on a microfluidic chip using nanoliter-size droplets. *J. Am. Chem. Soc.* 125:11170–11171.
38. Garcia, E., S. Veesler, R. Boistelle, and C. Hoff. 1999. Crystallization and dissolution of pharmaceutical compounds an experimental approach. *J. Cryst. Growth.* 198/199:1360–1364.